Available online at www.sciencedirect.com
SCIENCE DIRECT®
Journal of Nuclear Materials 329–333 (2004) 442–446
journal of nuclear materials
www.elsevier.com/locate/jnucmat

Effects of purity on high temperature mechanical properties of vanadium alloys

M. Koyama *, K. Fukumoto, H. Matsui

IMR/Tohoku University, 2-1-1 Katahira, Aoba-ku, Sendai 980-8577, Japan

Abstract

Creep tests of highly purified V–4Cr–4Ti alloy (NIFS-Heat) and V–10Cr–5Ti were examined using a purification technique of Zr heat treatment. The creep strain rate for highly purified specimens from the Zr-treatment was higher than for the original specimens. The effect of dynamic strain aging almost disappeared in the highly purified NIFS-Heat alloy containing less than 10 wppm oxygen. The result of the dissolution of precipitate bands and precipitates and removal of interstitial impurities was a decrease in the flow stress and ultimate tensile stress and a decrease of creep strength. These occurred at temperatures where the effect of dynamic strain aging can be seen in specimens containing above 170 wppm oxygen. The strain rate sensitivity parameters at a flow stress at 8% were negative even in highly purified NIFS-heat alloys, however their values were smaller than for specimens containing 150 wppm oxygen, and for data from previous work.

1. Introduction

V–4Cr–4Ti alloys are attractive for fusion reactor systems because they exhibit low neutron-induced activation, high resistance to swelling and good thermal and mechanical properties required for high temperature system performance [1,2]. But susceptibility of vanadium base alloys to low temperature embrittlement during neutron irradiation may limit the application of these alloys in low temperature ($\sim<$ 430 °C) regimes. The radiation-induced loss of ductility at $<$ 400 °C may be attributed to fine precipitates containing interstitial impurities [3–5]. The reduction of impurities is expected to improve the radiation resistance of the alloys at low temperature. The National Institute for Fusion Science (NIFS), in collaboration with Japanese industry, has initiated a program to fabricate a large ingot of high purity V–4Cr–4Ti alloy [6–8]. On the other hand, precipitates containing interstitial impurities are useful for maintaining the high temperature creep strength of vanadium alloys. Moreover, it is known that oxygen in vanadium alloys is extracted by liquid lithium in a lithium–vanadium blanket system proposed for advanced fusion reactor. This may result in a decrease of the mechanical strength of vanadium alloys at high temperatures. Thus, alloying to compensate for this loss of creep strength may be necessary in high-purity vanadium alloys. It has been reported that the NIFS-Heat alloys of V–4Cr–4Ti exhibit no significant degradation of creep or tensile properties at elevated temperatures [9]. However, it is still unclear what critical concentration of impurities required to avoid the degradation of high temperature performance of V–4Cr–4Ti alloys. The objective of this study is to establish what reduction of interstitial impurities by ultra high-purification is allowed while still maintaining the high temperature performance of V–Cr–Ti alloys. It will also focus on the effects of high purity in V–Cr–Ti alloys on mechanical properties at high temperature, such as dynamic strain aging (DSA).

2. Experimental procedures

A NIFS-Heat2 of V–4Cr–4Ti alloy [7,8] and a V–10Cr–5Ti (V–10.9Cr–4.9Ti, C:20 wppm, O:450 wppm,

* Corresponding author. Tel.: +81-22 215 2067; fax: +81-22 215 2066.
E-mail address: masahiro@imr.edu (M. Koyama).

0022-3115/$ - see front matter © 2004 Published by Elsevier B.V.
doi:10.1016/j.jnucmat.2004.04.092

Table 1
A list of chemical composition for NIFS-Heat2 alloys after heat treatment

Chemical composition (wppm)		
	O	N
NIFS-H2 original	170	130
NIFS-H2 Zr-treated, 1000 °C	35	70
NIFS-H2 Zr-treated, 1100 °C	<10	10

The annealing period is 2 h for all heat treatment conditions.

N:10 wppm) alloy were used in this study. SSJ specimens ($16\times4\times0.25$ mm with a 1.2 mm$\times$5 mm gauge section) were used for tensile and creep tests. Specimens were punched from the sheets and annealed at 1000 °C for 2 h after a degassing treatment at 600 °C for 0.5 h in a vacuum of $<\sim1\times10^{-4}$ Pa. In order to reduce the impurity concentration in V–Cr–Ti alloys, a zirconium foil gettering treatment (Zr-treatment) was employed. A sheet of alloy was sandwiched between a pair of zirconium foils using Mo holders. The sandwiched specimens were annealed at temperatures between 1000 and 1100 °C for 2 h in vacuum. After annealing, the layer of zirconium was removed by chemical polishing. The tensile specimens were punched from the sheet and annealed at 600 °C for 1 h in order to remove any hydrogen picked up during chemical polishing [4]. Using this process, the impurity concentration in vanadium alloys was drastically reduced as shown in Table 1. It has been demonstrated that the annealing temperature can control the impurity concentration in unalloyed alloys for the Zr-treatment method [10]. Annealing at high temperature makes the diffusion of impurities activated thermally and the more impurities were scavenged from vanadium alloys to zirconium foils at the higher Zr-treatment temperature. For the 1100 °C Zr-treatment, oxygen and nitrogen concentrations were reduced below 10 and 20 wppm, respectively. Tensile tests were carried out at a strain rate of 6.67×10^{-4}/s at temperature ranging from room temperature to 800 °C in a vacuum of $<\sim1\times10^{-4}$ Pa. In order to get information of strain rate sensitivity (SRS)[11], tensile tests were conducted at temperatures between RT and 750 °C for strain rates in the range 6.67×10^{-4} to 6.67×10^{-2}/s. Creep tests were carried out on the same machine as the tensile tests, which was converted to a load-controlled configuration. The temperatures of creep tests were 700, 750 and 800 °C with applied stress levels of 150 and 200 MPa. The details of creep test were provided elsewhere [9].

3. Results

3.1. Creep tests

Fig. 1 shows a comparison of steady state creep rates for NIFS-Heat and V–10Cr–5Ti alloys at 800 °C as a function of stress. In Fig. 1, five types of specimens were examined in the creep test. Two types of NIFS-Heat alloy were adopted; 170 wppm oxygen concentration (conventional heat-treatment) and 10 wppm oxygen (Zr-treatment). Three types of V–10Cr–5Ti alloy were used; 450 wppm oxygen (original specimen) and 100 and 20 wppm (Zr-treatment). From Fig. 1, the strain rate of Zr-treated NIFS-Heat alloy was one order of magnitude larger than the original specimen. Comparing NIFS-Heat with V–10Cr–5Ti, the same strain rate of $3–4\times10^{-4}$/h was obtained at a stress level of 200 MPa for NIFS-Heat and 275 MPa for V–10Cr–15Ti. This shows that the addition of chromium is effective for improving the creep strength of V–Cr–Ti alloys. Fig. 1 shows the same increase of strain rate due to Zr-treatment purification in both V–10Cr–5Ti and NIFS-Heat V–4Cr–4Ti. Tensile tests for identical specimens to those used in creep tests also were examined at a strain rate of 6.67×10^{-4}/s. Fig. 2 shows the plot of ultimate tensile strength of NIFS-Heat2 and V–10Cr–5Ti alloys versus test temperatures. Some previous data for V–4Cr–4Ti is

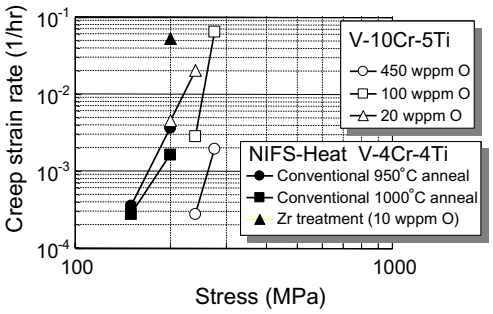

Fig. 1. Creep strain rate versus stress for original and Zr-treated specimens of NIFS-Heat and V–10Cr–5Ti alloys.

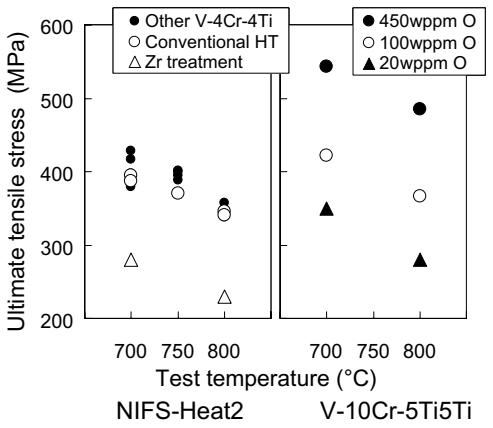

Fig. 2. Temperature dependence of ultimate tensile strength for NIFS-Heat2 and V–10Cr–5Ti alloys with a variety of oxygen concentration.

also plotted in Fig. 2. The data of original NIFS-Heat2 alloys was within the range of the date of previous work [9]. A large drop in UTS at high temperature can be seen for both Zr-treated NIFS-Heat2 alloy and V–10Cr–5Ti in Fig. 2. The decreases of UTS (Fig. 2) and yield stress (not shown) have a direct relationship to the decrease of creep strength. Therefore, the ultra high purification by Zr-treatment has reduced the tensile strength land lead to the degradation of creep properties for V–Cr–Ti alloys.

3.2. Tensile test

Tensile tests of original and Zr-treated NIFS-Heat2 alloy were performed at temperatures from RT to 800 °C. The yield stress and UTS of Zr-treated NIFS-Heat2 alloy were lower than original specimens, and the UTS data are shown in Fig. 2. Especially, there was a remarkable decrease of UTS in Zr-treated specimens at temperatures from 500 to 800 °C. Most stress–strain curves for original NIFS-Heat alloy exhibited Luders strain after the elastic regime. In the case of specimens with <70 wppm oxygen, however, both upper and lower yield points and Luders strain had completely disappeared in stress-strain curves at all temperatures.

Serrations in the flow stress in the stress strain curves were observed in the specimens tested at temperatures between 450 and 750 °C. Above 700 °C, discontinuous large drop serrations were observed on the stress strain curve after the stress reached the ultimate tensile strength. Fig. 3 shows the dependence of the serration amplitude on test temperatures for NIFS-Heat alloy. Amplitudes of serrations for Zr-treated specimens were smaller than ones for original specimens.

The SRS parameter, m, was determined from the flow stress measured at 8% strain for each temperature and strain rate. They were calculated from a logarithmic fit to the measured flow stress at 8% strain as a function of strain rate from 6×10^{-4} to 6×10^{-2} s. Fig. 4 shows the SRS parameter m as a function of test temperature for original and Zr-treated NIFS-Heat alloy. The m parameter was positive below 300 °C and above 600 °C for original NIFS-Heat alloy. Negative m parameter occurred in the temperature regime from 400 to 500 °C. On the other hand, the m parameter for Zr-treated NIFS-Heat alloy was negative at temperatures from 300 to 700 °C. The results for the original specimens were in good agreement with the temperature range of the appearance of serration behavior on the stress–strain curves. It indicated a correlation between the effect of DSA and the strain rate sensitivity, and that the interstitial impurities are related to the strain rate sensitivity [11–13].

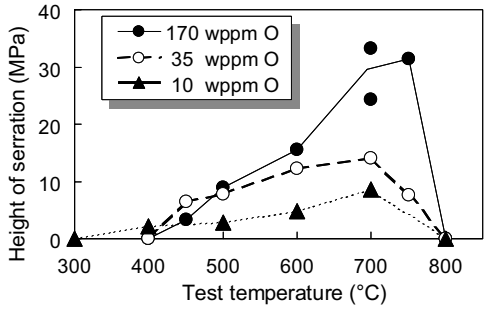

Fig. 3. Temperature dependence of amplitude of serration on flow stress in NIFS-Heat2 alloys.

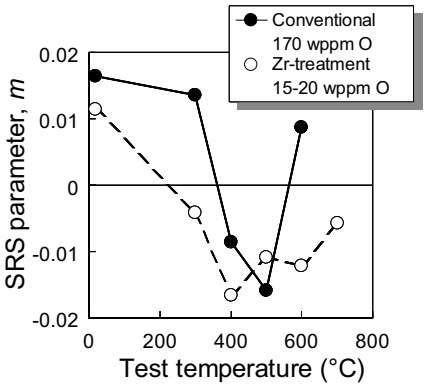

Fig. 4. Strain rate sensitivity parameter, m as a function of temperature for NIFS-Heat2, illustrating the effect of oxygen concentration.

4. Discussion

4.1. The effect of interstitial impurities on creep behavior of V–Cr–Ti alloys

The decrease of creep strength at high purity is related to the decrease of the ultimate tensile stress and yield stress. Especially in the temperature regime from 400 to 700 °C, the hardening caused by the effect of DSA is eliminated by the high purification of vanadium alloys. In order to investigate the microstructural changes that result from high purification, TEM observations were made for original and Zr-treated V–10Cr–5Ti specimens. Fig. 5 shows the microstructures in V–10Cr–5Ti alloys illustrating the effect of oxygen concentration. At 450 wppm oxygen, the precipitates of Ti(O,C,N) were formed homogeneously in the matrix and on the grain boundaries. When the oxygen concentration was lowered to 100 wppm, precipitates were formed heterogeneously in the grains and only scattered precipitates were seen on the grain boundaries. At 20 wppm oxygen, no precipitates of Ti(O,C,N) in the grains and on grain boundaries were observed in V–10Cr–5Ti.

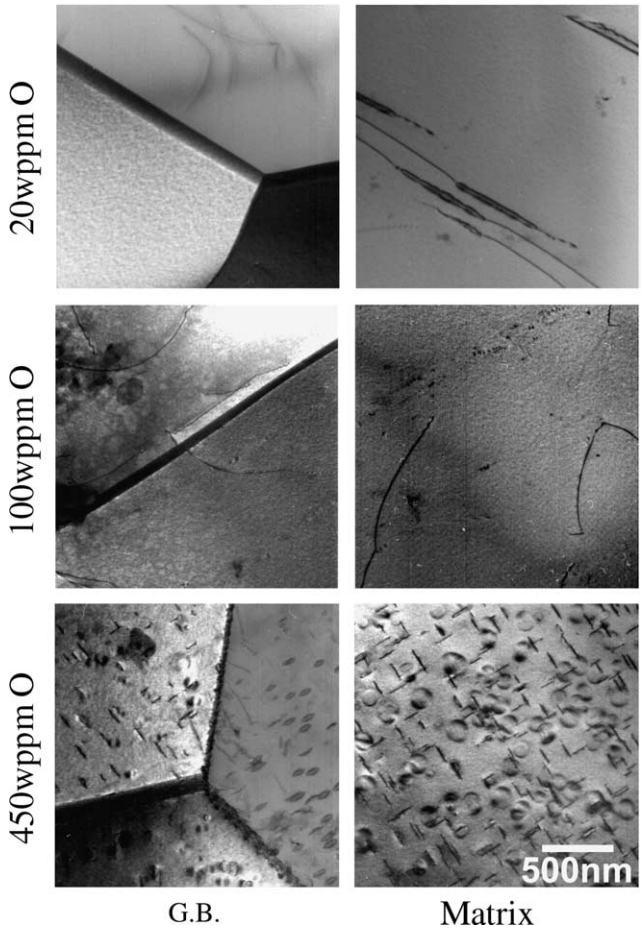

Fig. 5. TEM micrographs of V–10Cr–5Ti alloy illustrating the effect of oxygen concentration. Left micrographs correspond to microstructure at grain boundaries. Right ones show the microstructures in grain interiors.

The results of TEM observations indicate that microstructural changes affect the tensile behavior and creep properties of V–Cr–Ti alloys. In the previous study, it was reported that the thermal creep property of NIFS-Heat alloy is comparable to other V–4Cr–4Ti alloys and the impurity level (150–300 wppm) has little or no affect on the thermal creep properties of V–4Cr–4Ti. In this case, precipitate bands aligned in the rolling direction were observed in the NIFS-Heat2 alloys containing 170 wppm oxygen. The precipitation bands have been observed in vanadium alloys containing titanium at 300–1000 wppm oxygen. For V–10Cr–5Ti alloys, the density of precipitation bands decreased with decreasing impurities to 100 wppm oxygen. As a result of the decrease in the density of precipitation bands, the creep strain rate for Zr-treated specimens was higher than for the original specimens. The additional purification by Zr-treatment to 10 wppm oxygen strongly lowers creep properties in V–Cr–Ti alloys. When the oxygen concentration decreases due to increasing the annealing temperature during Zr-treatment, the precipitation bands and precipitates on the grain boundary are dissolved at first and then the impurities at interstitial site are removed by diffusion into the Zr foils. The increase of chromium in V–Cr–Ti alloys apparently did not affect the component of Ti(O,C,N) secondary phase and the characteristics of grain boundaries. The Cr addition provides strengthening as a substitutional solute in vanadium alloys. In order to compensate for the loss of creep strength due to high purification, the Cr addition is an effective method, as shown in Fig. 1. However it increases the radiation-induced embrittlement at low temperatures because of the significant hardening. It is necessary to optimize the chemical composition of V–Cr–Ti alloys for fusion reactor structural applications by balancing the high temperature performance by the Cr addition and the suppression of raising radiation-induced DBT by the high purification.

4.2. Changes of strain rate dependence by reduction of interstitial impurities

The SRS parameter, m of unalloyed vanadium was shown to have a negative temperature region 300 to 500 °C in previous work [14]. Because slip is a thermally activated process, the flow strength increases with increasing strain rate, i.e., m is generally positive. However, it has been reported that a negative SRS dependence of the flow stress can result from heterogeneous deformation processes since the diffusion of solute atoms to dislocations temporarily arrested at obstacles in the slip path occurs in the temperature regime of DSA. From Holtzer's work [13], the SRS parameter in V–4Cr–4Ti containing 300 wppm oxygen was negative in the temperature range 400–700 °C at strain rate from 10^{-5} to 10^{-1}. It was in good agreement with the present data of SRS parameter for original NIFS-Heat2 alloy. On the other hand, the Zr-treated NIFS-Heat alloy showed a wider negative temperature region of the SRS parameter than original specimens. The Zr-treated NIFS-Heat alloy had smaller amplitude of serration due to the effect of DSA than original specimens. This means that the effect of DSA was suppressed by the reduction of impurity content due to high purification. When the effect of DSA decreases and disappears, the SRS parameter should be converted to a positive value because the obstacles to dislocation movement are removed and the time available for solute diffusion to dislocations is extended [11]. The results of the SRS and the DSA behavior for highly purified NIFS-Heat alloy are clearly inconsistent. However the values of SRS for Zr-treated NIFS-Heat alloy were smaller than in Holtzer's work [13] and original NIFS-heat alloy. Besides, the flow stress dependence on test temperatures at strain rate of 6.67×10^{-4} s showed no change of flow stress from 300 to 700 °C [9] and flow stress curve were rather smooth, indicating a homogeneous deformation process. Further experimental data are required and the measurement of the SRS for highly purified unalloyed vanadium is planed as the next step.

Acknowledgements

This work was jointly funded by the collaboration program with the National Institute for Fusion Science.

References

[1] H. Matsui et al., J. Nucl. Mater. 233–237 (1996) 92.
[2] T. Muroga et al., J. Nucl. Mater. 307–311 (2002) 547.
[3] M. Satou, T. Chuto, et al., J. Nucl. Mater. 283–287 (2000) 367.
[4] K. Fukumoto, H. Matsui, et al., J. Nucl. Mater. 283–287 (2000) 535.
[5] P.M. Rice, S.J. Zinkle, J. Nucl. Mater. 258–263 (1998) 1414.
[6] T. Muroga, T. Nagasaka, et al., J. Nucl. Mater. 283–287 (2000) 711.
[7] T. Nagasaka, H.J. Heo, et al., Fusion Eng. Des. 61&62 (2002) 757.
[8] T. Nagasaka, T. Muroga, et al., Fusion Technol. 39 (2001) 659.
[9] K. Fukumoto, T. Yamamoto, et al., J. Nucl. Mater. 307–311 (2002) 610.
[10] K. Abe, K. Toma, et al., J. Less-Common Met. 23 (1971) 213.
[11] M. Zaiser, P. Hanher, Phys. Stat. Sol. (b) 199 (1997) 267.
[12] A.F. Rowcliffe, S.J. Zinkle, et al., J. Nucl. Mater. 283–287 (2000) 508.
[13] D.T. Hoeltzer, A.F. Rowcliffe, J. Nucl. Mater. 307–311 (2002) 596.
[14] R.W. Thompson, N. Carlson, J. Less-Common Met. 7 (1964) 321.